Received: 17 August 2021 | Revised: 19 October 2021 | Accepted: 28 November 2021

DOI: 10.1002/psp4.12751

ARTICLE

Translating *in vitro* CFTR rescue into small molecule correctors for cystic fibrosis using the Library of Integrated Network-based Cellular Signatures drug discovery platform

Matthew D. Strub[1,2] | **Shyam Ramachandran**[1] | **Dmitri Y. Boudko**[3] | **Ella A. Meleshkevitch**[3] | **Alejandro A. Pezzulo**[4] | **Aravind Subramanian**[5] | **Arthur Liberzon**[5] | **Robert J. Bridges**[3] | **Paul B. McCray Jr.**[1,2]

[1]Department of Pediatrics, University of Iowa, Iowa City, Iowa, USA

[2]Interdisciplinary Graduate Program in Genetics, University of Iowa, Iowa City, Iowa, USA

[3]Department of Physiology and Biophysics, Rosalind Franklin University, North Chicago, Illinois, USA

[4]Department of Internal Medicine, University of Iowa, Iowa City, Iowa, USA

[5]Broad Institute of MIT and Harvard, Cambridge, Massachusetts, USA

Correspondence
Paul B. McCray, Jr., Department of Pediatrics, University of Iowa, Carver College of Medicine, 169 Newton Road, Iowa City, IA 52242, USA.
Email: paul-mccray@uiowa.edu

Present address
Shyam Ramachandran, Sanofi, Waltham, Massachusetts, USA

Dmitri Y. Boudko and Ella A. Meleshkevitch, ReCode Therapeutics, Dallas, Texas, USA

Arthur Liberzon, Alkermes, Waltham, Massachusetts, USA

Funding information
National Institutes of Health RO1 HL118000, P01 HL51670, and P01 HL091842, the Center for Gene Therapy

Abstract

Cystic fibrosis (CF) is a lethal autosomal recessive disease caused by mutations in the cystic fibrosis transmembrane conductance regulator (*CFTR*) gene. The common ΔF508-CFTR mutation results in protein misfolding and proteasomal degradation. If ΔF508-CFTR trafficks to the cell surface, its anion channel function may be partially restored. Several in vitro strategies can partially correct ΔF508-CFTR trafficking and function, including low-temperature, small molecules, overexpression of miR-138, or knockdown of *SIN3A*. The challenge remains to translate such interventions into therapies and to understand their mechanisms. One approach for connecting such interventions to small molecule therapies that has previously succeeded for CF and other diseases is via mRNA expression profiling and iterative searches of small molecules with similar expression signatures. Here, we query the Library of Integrated Network-based Cellular Signatures using transcriptomic signatures from previously generated CF expression data, including RNAi- and low temperature-based rescue signatures. This LINCS in silico screen prioritized 135 small molecules that mimicked our rescue interventions based on their genomewide transcriptional perturbations. Functional screens of these small molecules identified eight compounds that partially restored ΔF508-CFTR function, as assessed by cAMP-activated chloride conductance. Of these, XL147 rescued ΔF508-CFTR function in primary CF airway epithelia, while also showing cooperativity when administered with C18. Improved CF corrector therapies are needed and this integrative drug prioritization approach offers a novel method to both identify small molecules that may rescue ΔF508-CFTR function and identify gene networks underlying such rescue.

Matthew D. Strub and Shyam Ramachandran contributed equally to this work.

This is an open access article under the terms of the Creative Commons Attribution-NonCommercial License, which permits use, distribution and reproduction in any medium, provided the original work is properly cited and is not used for commercial purposes.
© 2021 The Authors. CPT: *Pharmacometrics & Systems Pharmacology* published by Wiley Periodicals LLC on behalf of American Society for Clinical Pharmacology and Therapeutics.

of Cystic Fibrosis P30 DK54759, and the Cystic Fibrosis Foundation. We acknowledge the support of the In Vitro Models and Cell Culture Core, the Roy J. Carver Charitable Trust (P.B.M.) and Training Grant T32GM008629 (M.D.S.)

Study Highlights

WHAT IS THE CURRENT KNOWLEDGE ON THE TOPIC?

Although several CFTR modulators have been developed, a substantial treatment gap remains and many patients with cystic fibrosis (CF) would benefit from improved corrector or other targeted therapies. Therefore, there is a need for additional modulator therapies to maximize pulmonary health in people with CF. Several in vitro strategies to correct ΔF508-CFTR have been identified, including overexpression of miR-138, knockdown of *SIN3A*, and low temperature.

WHAT QUESTION DID THIS STUDY ADDRESS?

By querying genomic signatures associated with rescue of CFTR in Library of Integrated Network-based Cellular Signatures, we aimed to identify small molecules to restore function to the ΔF508-CFTR protein and elucidate the mechanisms of efficacious molecules.

WHAT DOES THIS STUDY ADD TO OUR KNOWLEDGE?

We identified eight small molecules that restored partial function to ΔF508-CFTR in a cell culture model, including XL147, which was shown to rescue ΔF508-CFTR in cells from four donors. Post hoc analysis indicated that ribosomal stalk proteins may be involved in XL147-mediated CFTR rescue and subsequent experiments identified several genes, including RPL32, that contribute to CFTR rescue when knocked down.

HOW MIGHT THIS CHANGE DRUG DISCOVERY, DEVELOPMENT, AND/OR THERAPEUTICS?

This study supports a transcriptomic signature approach to identifying and repurposing drugs for the treatment of CF lung disease, while also providing lead compounds and genetic targets for the development of CF therapies.

INTRODUCTION

Cystic fibrosis (CF) is a lethal autosomal recessive disease caused by mutations in the CF transmembrane conductance regulator (*CFTR*) gene.[1] The most common CFTR mutation, termed ΔF508, causes protein misfolding, resulting in proteasomal degradation. If ΔF508-CFTR is allowed to traffic to the cell membrane, anion channel function may be partially restored, although the residency and open-state probability of the mutant protein are reduced.[2,3] As ~90% of patients with CF have at least one ΔF508 allele, there is substantial interest from academic and industry laboratories in identifying interventions that might restore function to this misprocessed protein.[4] To this effect, we previously reported that transfection with an miR-138 mimic or knockdown of *SIN3A* in polarized primary cultures of CF airway epithelia increased ΔF508-CFTR mRNA and protein levels, promoted trafficking of the mutant protein to the membrane, and partially restored cAMP-stimulated chloride conductance.[5] Additionally, Denning and colleagues reported that ΔF508-CFTR processing reverts toward that of wild-type CFTR during low temperature incubation.[2]

However, a challenge remains to translate such interventions into therapies and to understand their mechanisms. One approach for connecting such interventions to small molecule therapies that have previously succeeded for CF and other diseases is through the use of mRNA expression profiling and iterative searches for small molecules with similar expression signatures. The Connectivity Map (CMAP) is a comprehensive catalog of gene expression profiles from cultured human cells treated with bioactive small molecules, with pattern-matching algorithms to mine these data.[6] We previously used a transcriptomics-based drug discovery approach by using CMAP (build 02) to identify drugs that mimicked the miR-138 overexpression and *SIN3A* knockdown treatments.[7] Signatures generated in Calu-3 epithelia treated with a miR-138 mimic or *SIN3A* Dicer-Substrate Short Interfering RNAs (DsiRNAs) matched signatures of 27 small molecules. We reported the identification of four small molecules that partially restored ΔF508-CFTR function in primary CF airway epithelia. Of these, pyridostigmine showed cooperativity with corrector compound 18 (C18) in improving ΔF508-CFTR function, highlighting the utility of a transcriptomic signature approach in drug discovery. CMAP has also been used to successfully investigate multiple cancers, inflammatory bowel disease, and human skeletal muscle atrophy.[8–11] These studies provide support for the use of connectivity mapping to link gene expression, disease, and small molecule therapeutics.

Build 02 of CMAP, which we used in our initial connectivity mapping study, housed ~7000 gene expression profiles representing over 1300 compounds tested in three cell lines at multiple doses and durations. More recently, the Library of Integrated Network-based Cellular Signatures (LINCS) was introduced, which now contains over 3,000,000 gene expression signatures collected from the treatment of ~33,000 small molecules and ~9200 genetic perturbagens (shRNA, cDNA, and CRISPR) on over 200 cell types.[12] To produce such high-scale data, the CMAP team developed the L1000 platform, a rapid high-throughput gene expression profiling technology, which computationally converts raw fluorescence into gene expression signatures that can be queried using the LINCS software.[13] In this study, we further expanded and improved our transcriptomics-based drug discovery pipeline by including low temperature treatment signatures in our query and using the more robust LINCS drug discovery platform.

METHODS

Generation of gene sets and queries of the LINCS database

Differential gene expression analysis was performed using the Partek Genomics Suite Gene Expression (St. Louis, MO) workflow to identify the most significant up- and downregulated genes. A p value cutoff less than 0.02 and fold change greater than 1.2 gave roughly 200 genes in each category, which were uploaded on to the internal LINCS database, at the time not publicly available. Every reference signature in the database was compared with the query signatures and given a score termed the "connectivity score" based on the extent of similarity between the two. Scores range from +1 (indicating higher similarity) to 0 (no similarity) and to −1 (meaning that the two signatures are opposite of each other). Candidate drugs with a connectivity score nearest to +1 were selected. LINCS also used stringent controls, as well as biological and technical replicates, in all experiments. These included: (1) correlation coefficient across replicates, (2) signal strength measured as the ratio of the top 50 and bottom 50 expressed genes, and (3) correlation of rank, determined by examining the percent correlation of differentially expressed genes between the replicates (Tables S1–S3). Candidate drugs with a favorable score in all three factors, a positive enrichment score (drugs that most closely mimicked our interventions), and the highest relative frequency (prioritizes the most important hits by controlling for variability in sampling size) were prioritized for further screening. The top 75 compounds for each query were included in the initial list before duplicates and unavailable compounds were removed, resulting in a final list of 107 small molecules.

Small molecules

Small molecules were obtained from the Broad Institute DOS Library (Cambridge, MA, USA), Cayman Chemical (Ann Arbor, MI, USA), or Sigma-Aldrich (St. Louis, MO, USA). For detailed information on small molecules, see Table S4.

Cultured cells

The CF bronchial epithelial cell line CFBE41o$^-$, hereafter termed "CFBE," was originally developed by immortalization of human CF airway cells and later stably transduced with a ΔF508-CFTR expression cassette. These cells were cultured as previously described.[14–16] Primary human airway epithelia were cultured as previously described.[17]

Functional screen of compound activity by conductance assay

Effects of selected compounds were tested using the robotic Transepithelial Current Clamp TECC-24 assay (EP Design, Bertem, Belgium) with CFBE cells grown on microporous membranes of Transwell plates (Corning, Corning, NY, USA), representing a planar array of 24 Ussing chambers with a 6 mm diameter insert containing the epithelial monolayer. Cells were pretreated 24 h before experiments with Log-titrated and 0.2% DMSO-normalized compounds with and without 3 μM C18 (1, 3, 10 μM final concentrations in 250 μl apical +750 μl basolateral solution, incubated at 37°C). An addback treatment was performed 90 min prior to the start of electrophysiology experiments. The 10 μM C18 and 0.2% DMSO were used as positive and negative controls, respectively. Drugs were tested in duplicates and controls in triplicates. For CFBE cells, baseline sodium conductance was suppressed by the apical addition of 3 μM benzamil prior to transepithelial current analysis. After 20 min of baseline measurements, CFTR-dependent chloride conductance was stimulated with the apical and basolateral addition of 10 μM forskolin and 1 μM ivacaftor (Vertex Pharmaceuticals, Boston, MA, USA), followed by 20 μM Inh-172-induced CFTR inhibition

60 min later. The area under the curve (AUC) of chloride conductance was calculated for the 60-min interval between additions of 10 μM forskolin and 1 μM ivacaftor (20 min mark) and 20 μM Inh-172 (80 min) for all small molecules.

Transepithelial chloride current studies

Transepithelial chloride current measurements were made in Ussing chambers ~10 days post-seeding. Briefly, primary cultures were mounted in the Ussing chamber and transepithelial chloride current was measured under short-circuit conditions. After measuring baseline current, the transepithelial current (I_t) response to sequential apical addition of 100 μM amiloride, 100 μM 4,4′-diisothiocyanoto-stilbene-2,2′-disulfonic acid (DIDS), 10 μM forskolin and 100 μM 3-isobutyl-1-methylxanthine (IBMX), and 100 μM GlyH-101 was measured. Studies were conducted with a chloride concentration gradient containing 135 mM NaCl, 1.2 mM $MgCl_2$, 1.2 mM $CaCl_2$, 2.4 mM K_2PO_4, 0.6 mM KH_2PO_4, 5 mM dextrose, and 5 mM Hepes (pH 7.4) on the basolateral surface, and gluconate substituted for chloride on the apical side.

Statistical analysis

For conductance studies, the AUC of transepithelial conductance measurements between the additions of 10 μM forskolin and 1 μM ivacaftor and 20 μM Inh-172 were calculated. AUC ratios were computed for small molecule-treated replicates relative to the mean AUC of control experiments. Experiments with a baseline transepithelial resistance less than 400 $G{\cdot}cm^2$ were considered toxic and removed from further analyses. One sample, one-sided *t*-tests were performed to evaluate whether small molecule AUC ratios were greater than control AUC ratios, with Benjamini-Hochberg multiple hypothesis adjustment applied to the results of each small molecule. The AUC thresholds were established based on experience from other small molecules screened at Rosalind Franklin University for rescue of ΔF508-CFTR.[18] A stringent threshold of AUC greater than 1.25 was used for the initial screen. Data are presented as a mean ± SE of individual data points. Adjusted (adj) $p < 0.05$ was considered significant. For chloride current studies, the average change in peak transepithelial current (I_t) was calculated and statistical significance was determined by one sample, one-sided *t*-tests with Benjamini-Hochberg multiple hypothesis adjustments (adj $p < 0.05$).

RNA-sequencing

Total RNA was isolated from CFBE cells using the *mir*Vana miRNA isolation kit (Ambion, Austin, TX, USA). Total RNA was tested on an Agilent Model 2100 Bioanalyzer (Agilent Technologies, Santa Clara, CA, USA). Samples with an RNA integrity number (RIN) greater than 8.0 were selected for further processing. Libraries were prepared using the TruSeq RNA Sample Prep (Illumina, San Diego, CA, USA) and submitted to the Iowa Institute of Human Genetics Genomics Division for deep sequencing. Data were processed using Kallisto and Sleuth.[19,20]

Network analysis

A STRING network consisting of CFTR as the central hub, 250 max interactors in the first shell, and 10 max interactors in the second shell was extracted from string-db.org.[21] This network had an interaction score of 0.400 and included all interaction sources. Transcripts per million (TPM) values for genes with an average TPM greater than 1 in XL147 and/or DMSO were inputted along with the STRING network into the DeMAND (Detecting Mechanism of Action based on Network Dysregulation) algorithm with default parameters. The code used for the DeMAND analysis is available at https://github.com/matthewdstrub/XL147. A detailed description of the DeMAND algorithm can be found in ref. 22

Oligonucleotide reagents

DsiRNAs were obtained as TriFECTa kits from IDT (Coralville, IA), each containing three pre-designed DsiRNAs per gene (Table S5). To ascertain the specificity of the oligonucleotides, we harvested RNA from cells transfected with the three pooled oligonucleotides per gene and measured the expression of multiple genes. RNA was harvested from each sample 24 h post-transfection. First-strand cDNA was synthesized using SuperScript II (Invitrogen, Waltham, MA, USA), with oligo-dT and random-hexamer primers. Primers for each gene were designed and produced by IDT and validated in HEK cells. Quantitative real-time polymerase chain reaction (RT-PCR) was performed using the QuantStudio 6 Flex Real-Time PCR system (Applied Biosystems, Waltham, MA, USA). All experiments were performed in quadruplicate. Following validation of knockdown efficiency, three DsiRNAs per gene were pooled and CFBE cells were reverse-transfected using Lipofectamine RNAiMAX (Invitrogen) and grown on microporous membranes of Transwell plates 120 h prior to the electrophysiology measurements.

RESULTS

Identification and screening of candidate small molecules using the Library of Integrated Network-based Cellular Signatures

Microarray signatures generated in CFBE cells treated with miR-138 mimic, SIN3A DsiRNA, or low temperature (27°C; Gene Expression Omnibus Series GSE142610) were used to generate gene sets, consisting of up- and downregulated genes, to query LINCS.[23] Candidate small molecules with signatures closely mimicking those of our queries, strong correlation across replicates, signal strength, and conservation across a minimum of two treatments were prioritized in this study (Tables S1–S3). We screened 107 small molecules (Table S4) for functional rescue of ΔF508-CFTR in CFBE cells. CFBE cells were basolaterally and apically treated with compounds of interest for 24 h, with addback performed 90 min prior to electrophysiological measurements. Small molecules were tested at three concentrations (1, 3, and 10 μM) and in the presence or absence of C18, an analog of VX-809 (Lumacaftor; Vertex Pharmaceuticals). Five molecules showed significant activity (A893, K659, K750, Dorsomorphin, and XL147; Figure 1a) with four also showing synergistic rescue with C18 (all except A893; Figure 1b).

We next screened an additional 28 small molecules (Table S6) that were chemically related to the five active molecules identified (Figure 1a,b), with the rationale being that the active molecules represent an efficacious structure or residue, or target a specific pathway. Twenty relatives were structural congeners of the active molecules. Because XL147 is a member of the PI3K inhibitor drug class, an additional eight small molecule inhibitors of PI3K were also tested. Treatment with three congeners of K659 significantly increased transepithelial chloride conductance in CFBE cells (Figure 1c), while also showing synergistic rescue in combination with C18 (Figure 1d).

Testing of efficacious compounds in primary human airway epithelia

After screening 135 small molecules in CFBE cells, we identified eight active molecules that significantly rescued ΔF508-CFTR transepithelial chloride conductance. Next, we selected small molecules with an AUC ratio of 1.25 or greater (i.e., a 25% or greater increase in conductance), which we considered to be the threshold of substantial activity, for testing in primary human airway epithelia. All eight molecules were subsequently tested in well-differentiated primary human airway epithelia from a single ΔF508/ΔF508-CFTR donor (Table S7), with six showing significant improvement in ΔF508-CFTR-mediated transepithelial chloride conductance in at least one of our experimental regimens (i.e., alone or in combination with C18; Figure 2a,b). Two of the small molecules produced AUCs greater than 1.25; dorsomorphin was efficacious alone (Figure 2c), whereas XL147 showed activity alone and in the presence of C18 (Figure 2c,d). Dorsomorphin and XL147 were further tested in primary airway epithelia from four additional ΔF508/ΔF508-CFTR donors. XL147 had an average increase of 94.9% in peak chloride current after the addition of forskolin and Ivacaftor compared to DMSO. When in combination with C18, XL147 had a 56.5% increase compared to C18 alone (Figure 3). Dorsomorphin did not significantly improve chloride current compared to controls in these donors.

RNA-sequencing analysis of XL147

Following the identification of XL147 as an efficacious modulator of ΔF508-CFTR in multiple primary human airway epithelia donors, we performed RNA-sequencing of CFBE cells treated for 24 h with XL147 at its most effective concentration (3 μM). RNA from CFBE cells treated with the negative control (0.2% DMSO) and positive control (6 μM C18 and 5 μM VX-809) treatment groups were also sequenced. XL147 treatment resulted in 464 significantly upregulated genes and 169 significantly downregulated genes at false-discovery rate (FDR) less than 0.05. The 50 most upregulated and downregulated genes ranked by FDR are highlighted in Tables S8 and S9, respectively.

RNA-sequencing analysis of C18-treated CFBE cells revealed that only seven genes were differentially expressed when compared to DMSO. *SLC38A2*, *SLC7A11*, *AMIGO2*, *PHLDA1*, *CYP1B1*, *DKK1*, and *ABCG2* were all significantly upregulated, whereas no genes were downregulated. Likewise, only nine genes were differentially expressed in VX-809 treated CFBE cells compared to DMSO. *HR*, *PHLDB2*, *STC2*, *INHBA*, *OGT*, and *TENM3* were significantly upregulated, whereas *HIST2H2BE*, *SUOX*, and *PLK4* were significantly downregulated. The low number of genes with altered expression in C18 and VX809 strongly suggests that these corrector compounds are unlikely to act primarily through a transcriptional mechanism.

Network analyses of XL147

To elucidate the possible mechanisms of XL147's effects on ΔF508-CFTR, our RNA-sequencing data were

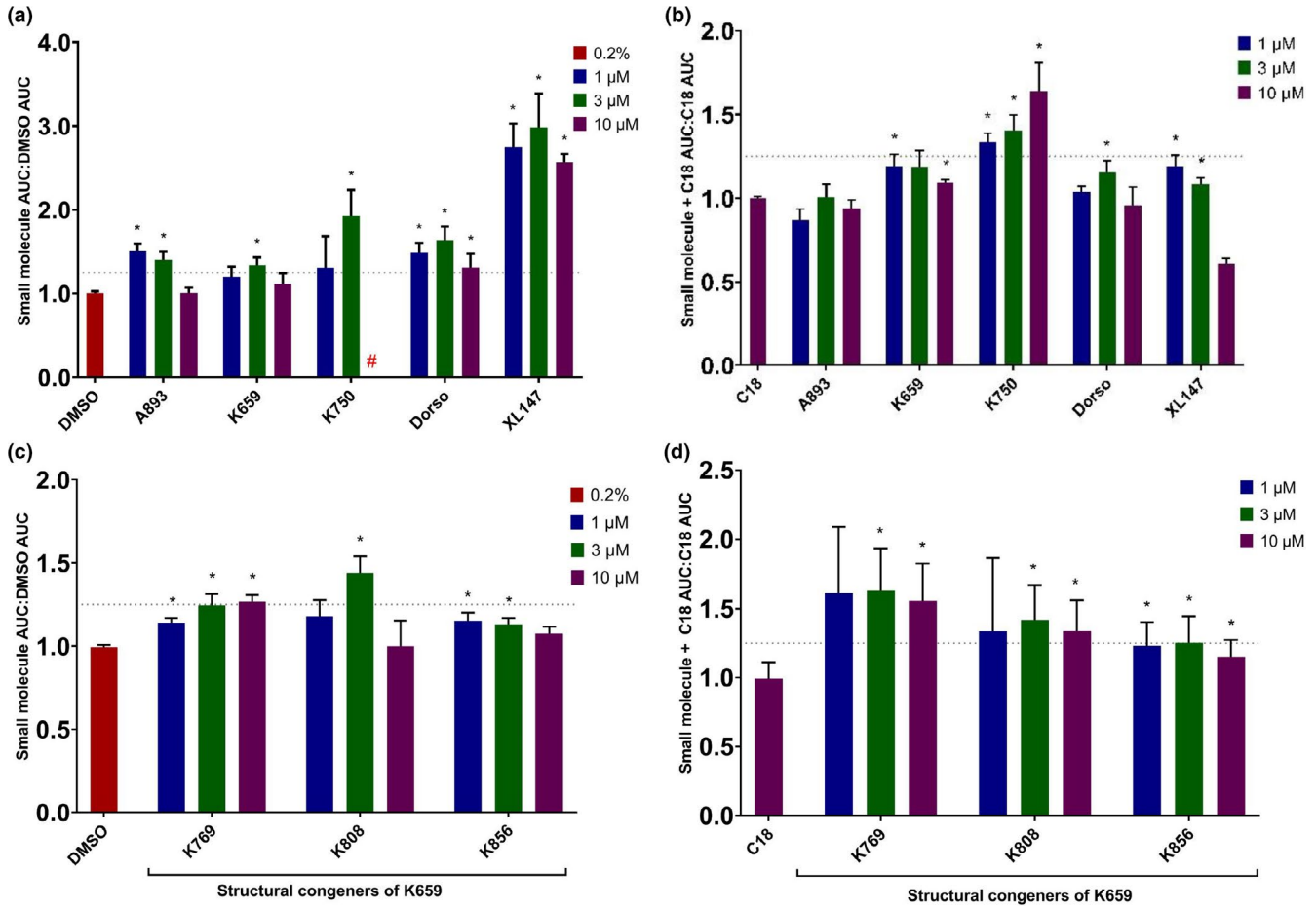

FIGURE 1 Eight small molecules rescue ΔF508-cystic fibrosis transmembrane conductance regulator (CFTR) function in cystic fibrosis bronchial epithelia (CFBE) cells. Transepithelial conductance (G_t) in response to forskolin and ivacaftor (F&I) and the CFTR inhibitor-172 (inh-172) under open circuit conditions was measured in polarized CFBE (ΔF508/ΔF508) cells using the TECC-24 assay. The area under the curve (AUC) of transepithelial conductance measurements between the additions of F&I and inh-172 were calculated. The ratio of the AUC of compound-treated cells compared to the AUC of DMSO-treated cells are displayed for active small molecules identified by (a) the original LINCS screen and (c) relatives of the original LINCS hits. The ratio of the AUC of cells treated with compounds in the presence of C18 compared to cells treated with only C18 are displayed for active small molecules identified in (b) the original LINCS screen and (d) relatives of the original LINCS hits. Small molecules were administered basolaterally for 24 h and addback of molecules was performed 90 min prior to the electrophysiology assay. Concentrations of small molecules are noted in the keys. DMSO was administered at 0.2% concentration and C18 was administered at 10 μM when used as a control and 3 μM when used in combination with candidate small molecules. *n* greater than or equal to four for all tested conditions. Error bars indicate standard error of the mean. *Indicates adjusted *p* value less than 0.05. #Indicates toxicity at noted concentration. Gray dotted line represents the threshold AUC ratio of 1.25. Relationships of molecules to parent compounds are noted under brackets in panels c and d. Note the difference in Y-axis scales across panels

run through Gene Set Enrichment Analysis (GSEA). Enriched hallmark terms with FDR q-value less than 0.25 for XL147 treatment included TGF-β signaling, apical surface, and PI3K/AKT/mTOR signaling (Table 1). Downregulated terms included large ribosomal subunit and immune response in mucosa. To further identify specific genes involved in XL147-mediated ΔF508-CFTR rescue, we used the Detecting Mechanism of Action by Network Dysregulation (DeMAND) algorithm. Briefly, we inputted our XL147 and DMSO RNA-sequencing profiles, as well as a CFTR-centric regulatory network from the STRING protein-protein interaction (PPI) networks database. DeMAND evaluated the dysregulation of each PPI by first using a Gaussian Kernel method to smooth the dysregulation co-expression scatterplots for any two interacting genes, generating interaction probability densities. Next, the density differences pre- and post-XL147 treatment were evaluated using KL-divergence and the statistical significance of each KL-divergence was assessed by gene pair shuffling. Last, the global dysregulation of each individual gene was determined by integrating the *p* values of all its network interactions. The DeMAND output yielded a rank-ordered list of potential genes contributing to the mechanism of XL147

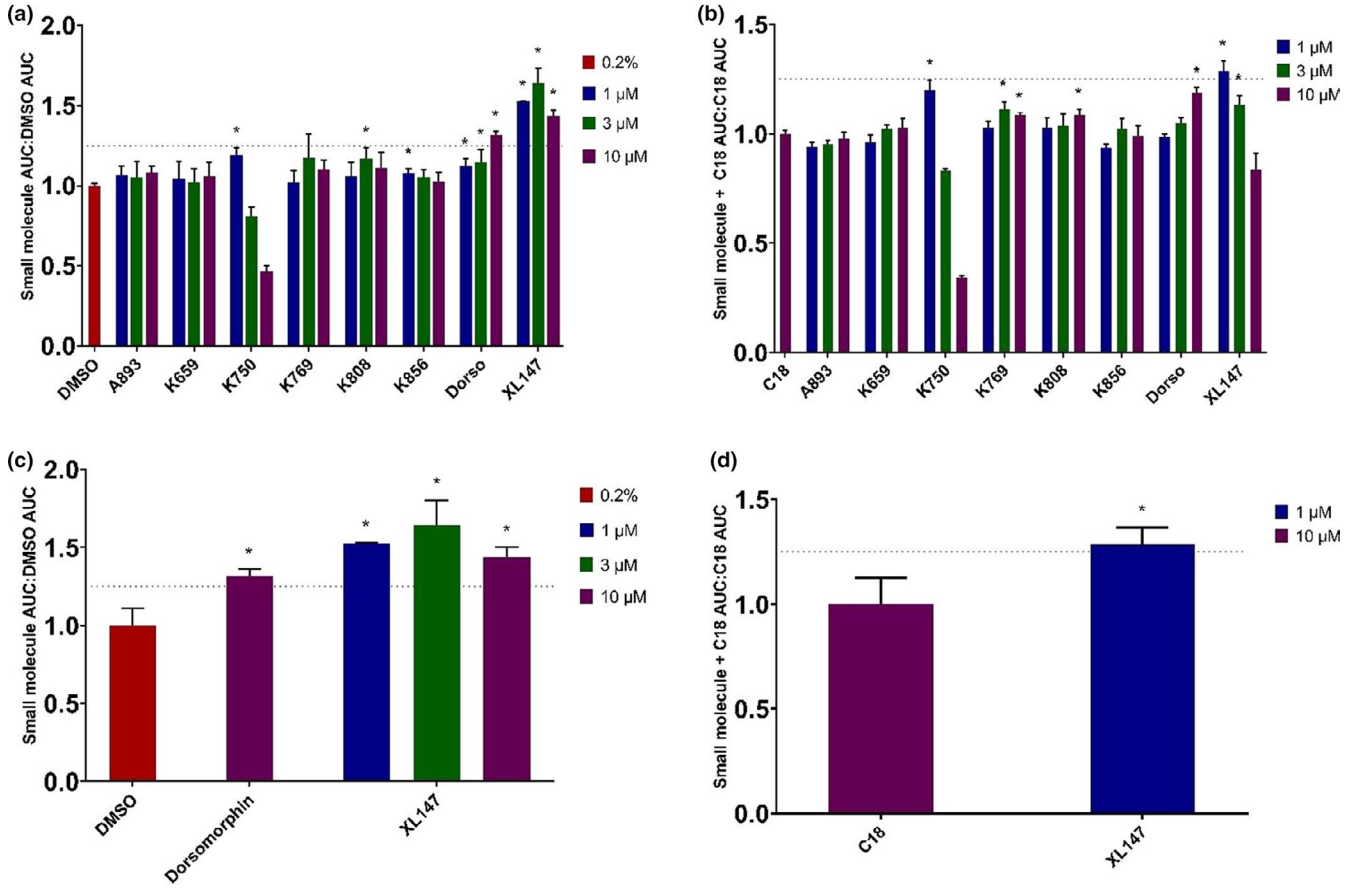

FIGURE 2 Six small molecules rescue ΔF508-cystic fibrosis transmembrane conductance regulator (CFTR) function in primary human airway epithelial cells from an individual ΔF508/ΔF508-CFTR donor. Transepithelial conductance (G_t) in response to forskolin and ivacaftor (F&I) and inhibitor-172 (inh-172) under open circuit conditions was measured in well-differentiated primary ΔF508/ΔF508 human airway epithelial cells using the TECC-24 assay. The area under the curve (AUC) of transepithelial conductance measurements between the additions of F&I and inh-172 were calculated. The ratio of the AUC of compound-treated cells compared to the AUC of control-treated cells are displayed for small molecules that showed efficacy in the absence (a) or presence (b) of C18. Compounds with an AUC greater than or equal to 1.25 in the absence or presence of C18 are displayed in panels c and d, respectively. Small molecules were administered basolaterally for 24 h and addback of molecules was performed 90 min prior to the electrophysiology assay. Concentrations of small molecules are noted in the keys. DMSO was administered at 0.2% concentration and C18 was administered at 10 μM when used as a control and 3 μM when used in combination with candidate small molecules. *n* greater than or equal to four technical replicates for all tested conditions. Error bars indicate standard error of the mean. *Indicates adjusted *p* value less than 0.05. Gray dotted line indicates AUC ratio of 1.25. Note the difference in Y-axis scales across panels

(Table S10). Numerous genes related to the large ribosomal subunit appeared in this output. As this GSEA hallmark term was downregulated in XL147 (Table 1), we hypothesized that knockdown of ribosomal-related proteins could increase ΔF508-CFTR trafficking to the cell surface and restore partial function.

siRNA-mediated knockdown of ribosomal stalk proteins rescues ΔF508-CFTR

We used pools of three DsiRNAs per gene to knockdown ribosomal stalk and other ribosome-related genes in CFBE cells. Interestingly, knockdown of *RPL32*, *RPL5*, *RPL9*, and *RPS8* resulted in significant restoration of transmembrane chloride current in ΔF508-CFTR CFBE cells (Figure 4). Of these, knockdown of *RPL32* yielded the greatest rescue, with an increase of 168.9% in peak chloride current after the addition of forskolin and IBMX compared to DMSO. Knockdown of *RPL32* also showed an increase of over 50% in peak chloride current when compared to knockdown of *SYVN1*. As Lukacs and colleagues previously identified *RPL12* as a CFTR modifier, we used knockdown of *RPL12* as an additional positive control.[24] When compared to *RPL12* knockdown, cells treated with the *RPL32* DsiRNAs showed an increase in peak chloride current of 54.6%.

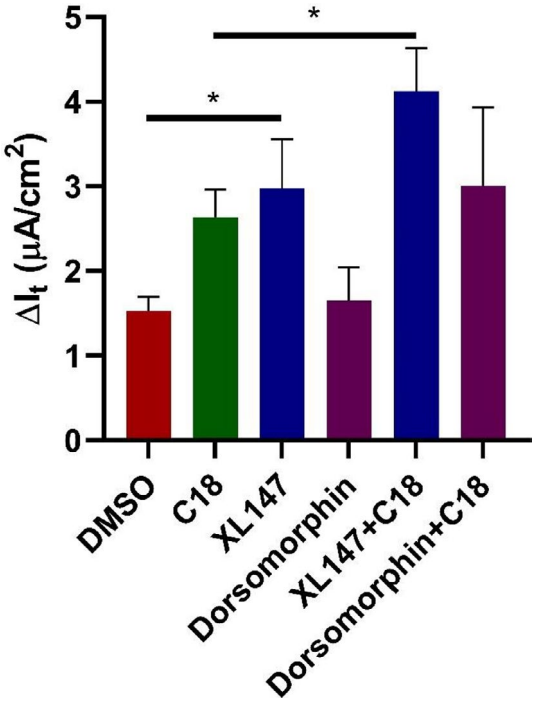

FIGURE 3 XL147 rescues ΔF508-CFTR function in primary human airway epithelial cells. Average change in transepithelial current (I_t) in response to forskolin and IBMX (F&I) and GlyH-101 under short circuit conditions was measured in well differentiated primary ΔF508/ΔF508 human airway epithelial cultures from four donors. Small molecules were administered basolaterally for 24 hs prior to the electrophysiology measurements in Ussing chambers. XL147 was administered at 3 μM, Dorsomorphin at 10 μM, C18 at 6 μM, and DMSO at 0.2%. Error bars indicate standard error of the mean. *Indicates adjusted *p* value less than 0.05

DISCUSSION

Since the discovery of the *CFTR* gene in 1989, great progress has been made in both the development of therapeutics for CF and the understanding of CFTR biogenesis. In 1992, Denning and colleagues discovered that ΔF508-CFTR is temperature sensitive and provided proof-of-principle that mutant CFTR could escape proteasomal degradation and retain partial function.[2] With this knowledge and the advent of high-throughput screening technologies, several small molecule CFTR modulators have been investigated for therapeutic purposes. The first US Food and Drug Administration (FDA) approved small molecule for the correction of ΔF508-CFTR was VX-809, which showed modest efficacy in clinical trials.[25] Recently, the triple combination therapy of elexacaftor-tezacaftor-ivacaftor (Trikafta; Vertex Pharmaceuticals) was FDA-approved and this three drug combination shows greater efficacy than VX-809.[26] However, despite an average increase of 13.8% in the forced expiratory volume in one second (FEV_1) in patients with one ΔF508 allele and a minimal-function mutation on the second allele, the improvement in lung function does not reach the levels observed in carriers of CFTR mutations.[27,28] Furthermore, nearly one-third of ΔF508 homozygotes experience less than a 5% increase in FEV_1 on Trikafta and some individuals do not tolerate the medication.[29] Unfortunately, CF remains progressive and fatal and improved treatments are needed. Likewise, the CFTR interactome remains incompletely understood and the identification of CFTR effectors could lead to improved therapeutics.

We previously reported that knockdown of SIN3A or overexpression of miR-138 rescues ΔF508-CFTR to the cell surface and restores partial function.[5] However, translating these discoveries into therapies remains a challenge, as the efficient delivery of siRNAs or microRNA mimics to airway epithelia is difficult.[30] Therefore, we attempted to connect such interventions to small molecule therapies via mRNA expression profiling. Our strategy was to identify small molecule-induced gene expression responses that were similar to the expression induced by SIN3A knockdown, miR-138 overexpression, or low temperature incubation. Such genomic signature strategies have previously worked for other diseases, including muscle atrophy, inflammatory bowel disease, and various cancers.[8,10,11]

The present work expands upon our previous genomic signature approaches to prioritize and test compounds for rescue of ΔF508-CFTR trafficking and function. We previously queried genomic signatures for miR-138 overexpression and SIN3A inhibition in the CMAP and iteratively mined candidate drugs with similar effects on gene expression.[7] We reported that the treatment of human primary airway epithelia with seven of these small molecules improved ΔF508-CFTR trafficking greater than C18 at two or more doses. Four of the molecules also improved ΔF508-CFTR maturation in CFBE cells. Following the introduction of LINCS, we integrated gene expression and pathway information from a variety of sources and the subsequent query aided us in identifying an additional three compounds that restored function to CFTR in human primary CF airway epithelial cells homozygous for ΔF508.[18]

Likewise, Pesce et al. (2016) had previously queried gene expression signatures characterizing low temperature in CMAP and found that anti-inflammatory glucocorticoids increased mutant CFTR function in a bronchial epithelial cell line.[31] However, these glucocorticoids were found to be ineffective in primary bronchial epithelial cells. Our strategy differed from the Pesce et al. analysis in several ways. First, we performed pattern-matching using LINCS, which contained 3,000,000 expression signatures (compared to 7000 in CMAP) of 33,000 small molecules (1300 in CMAP), and 9200 genetic perturbagens in over 200 cell lines (3 in CMAP). Furthermore, to produce such high-scale data,

TABLE 1 GSEA results of XL147 RNA-sequencing data compared to DMSO

Term	*p* value	FDR q-value	Direction in XL147
Oxidative phosphorylation	0.0214	0.0920	Down
Organellar large ribosomal subunit	0	0.0936	Down
Deoxyribonucleotide biosynthetic process	0	0.0972	Down
Angiogenesis	0.0188	0.1846	Up
Epithelial mesenchymal transition	0	0.1853	Up
Hypoxia	0	0.1869	Up
IL2 STAT5 signaling	0.1356	0.1936	Up
Apical surface	0.0980	0.1951	Up
Myc targets, version 2	0.0311	0.2011	Up
PI3K AKT mTOR signaling	0.0198	0.2068	Up
Glycolysis	0.0523	0.2077	Up
IL6 JAK STAT3 signaling	0.0302	0.2156	Up
TNFα signaling via NFκB	0.0775	0.2172	Up
KRAS signaling up	0.0792	0.2217	Up
Interferon alpha response	0.1021	0.2251	Down
Apical junction	0	0.2317	Up
Innate immune response in mucosa	0	0.2367	Down

Abbreviations: FDR, false-discovery rate; GSEA, Gene Set Enrichment Analysis.

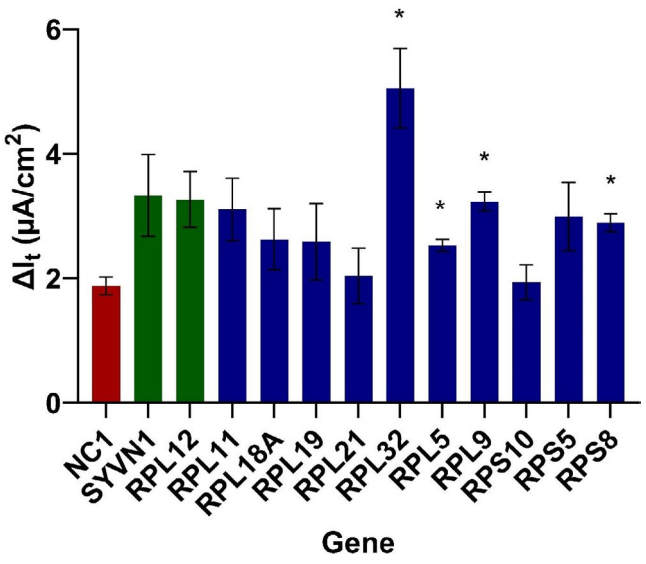

FIGURE 4 DsiRNA-mediated knockdown of ribosomal stalk proteins rescues ΔF508-CFTR function in CFBE cells. Average change in transepithelial current (I_t) in response to forskolin and IBMX (F&I) and GlyH-101 under open circuit conditions was measured in CFBE cells. Three DsiRNAs per gene were pooled and CFBE cells were reverse-transfected using Lipofectamine RNAiMAX and grown on microporous membranes of Transwell plates 120 h prior to the electrophysiology measurements. Error bars indicate standard error of the mean. *Indicates adjusted *p* value less than 0.05 when compared to DMSO. Knockdown of RPL32 also resulted in a statistically significant increase in transepithelial current compared to knockdown of positive controls RPL12 and SYVN1. $n = 4–5$ per candidate target gene. DsiRNAs, Dicer-Substrate Short Interfering RNAs

the L1000 rapid high-throughput gene expression profiling platform was developed and incorporated into the LINCS software. We reasoned that this considerable expansion of the LINCS dataset compared to its predecessor CMAP would enrich our chances of finding efficacious small molecules. Interestingly, we did not find that glucocorticoids were positively connected to the inputted low temperature signature (Table S3), resulting this ineffective drug class not being included in our candidate list. Second, we queried not only gene expression signatures characterizing low temperature, but also included signatures of miR-138 mimic and SIN3A DsiRNA, whose gene expression signatures differed greatly from low temperature, suggesting different mechanisms of rescue. Querying multiple forms of ΔF508-CFTR rescue also increased the likelihood of identifying correctors. Indeed, XL147 only appeared in the SIN3A DsiRNA output. By only querying low temperature, XL147 would not have been discovered. Last, we performed a more high-throughput screen, testing 135 small molecules compared to the 20 compounds investigated in the aforementioned study. Interestingly, Hegde et al. (2015) performed a reverse connectivity mapping experiment by extracting and deconvoluting the transcriptional profiles of ΔF508-CFTR proteostasis regulator drugs housed in CMAP to identify signaling cascades regulating proteostasis.[32] Although we used known sources of CFTR rescue to identify small molecule correctors, their approach used known correctors to identify genes or proteins involved in CFTR proteostasis. We adopted a similar approach

following the discovery of XL147, as we then performed RNA-sequencing on cells treated with XL147 and inputted the resulting transcriptomic data into the DeMAND algorithm to identify novel CFTR effectors.

In the current study, we queried high quality gene expression profiles of SIN3A knockdown, miR-138 overexpression, and low temperature incubation in a beta version of LINCS and identified eight out of 135 small molecules that partially restored chloride-mediated current in ΔF508-CFTR CFBE cells. This screen yielded an unusually high percentage of hits compared to traditional high-throughput screens and provided confidence in our approach.[33]

We focused on the small molecules that were most efficacious in CFBE cells for subsequent studies in primary epithelial cells. XL147 was found to partially restore CFTR-dependent chloride current to ΔF508-CFTR human primary airway epithelial cells from four donors. XL147 is a class 1 PI3K inhibitor that reversibly binds to lipid kinases in an ATP-competitive manner, thereby inhibiting the production of the secondary messenger PIP3 and preventing activation of the PI3K signaling pathway.[34] As activation of the PI3K pathway is frequently linked to tumorigenesis, XL147 has been investigated as an orally bioavailable cancer drug in several clinical trials for endometrial carcinoma, metastatic breast cancer, and glioblastoma (e.g., NCT01013324, NCT01042925, and NCT01240460; clinicaltrials.gov), although it has not yet been FDA approved. The PI3K/Akt/mTOR signaling pathway has also been targeted for the treatment of CF. Coppinger and colleagues used protein interaction profiling and global bioinformatic analyses to identify upregulation of mTOR activity in CFBE cells.[35] Inhibition of the PI3K/Akt/mTOR pathway with multiple unique inhibitors yielded an increase in CFTR stability and expression. Subsequent analyses determined that the most efficacious inhibitor, MK-2206, rescued ΔF508-CFTR by restoring autophagy, potentially through its presumed target BAG3. Additionally, Rotin and colleagues identified three small molecule inhibitors of the PI3K/Akt/mTOR signaling pathway (FPA-124, PI-103, and 10-DEBC) that restored partial short-circuit current and/or rescued CFBE maturation in ΔF508-CFTR MDCK and ΔF508-CFTR 293MSR-GT cells, respectively.[36] In a related study, Trzcinska-Daneluti and colleagues discovered that shRNA-mediated knockdown of FGF receptors (FGFRs) and downstream signaling proteins resulted in the partial rescue of ΔF508-CFTR maturation and surface stability. FGFRs are known activators of the PI3K/Akt/mTOR pathway. IPMK, a PI3K that acts as a molecular switch for Akt and can stimulate or inhibit PI3K/Akt signaling, was also identified as a suppressor of ΔF508-CFTR rescue.[37] Interestingly, how PI3K inhibition promotes rescue of ΔF508-CFTR is not fully known. Akt has been shown to promote cAMP-mediated trafficking of wild-type CFTR to the cell surface, although it has also been reported to decrease surface expression of plasma membrane proteins.[38–40] Whether XL147 rescues CFTR-mediated Cl^- current to ΔF508-CFTR via inhibition of the PI3K signaling pathway requires additional investigation. GSEA of our XL147 RNA-sequencing gene expression profile indicated an upregulation of PI3K/Akt/mTOR signaling, perhaps suggesting that XL147 is acting through an alternative mechanism. In addition, testing of several other PI3K inhibitors yielded modest results.

To further elucidate the potential mechanism of XL147, we used our RNA-sequencing data to query the DeMAND algorithm. The output consisted of a rank-ordered list of genes that could be mechanistically responsible for the activity of XL147. This list was enriched for ribosomal stalk proteins. RNAi knockdown of four candidates partially rescued chloride-mediated current in ΔF508-CFTR CFBE cells. Interestingly, Lukacs and colleagues identified a component of the ribosomal stalk, *RPL12*, as an effector of ΔF508-CFTR.[24] Silencing of *RPL12* attenuated the translational elongation rate and increased the folding efficiency and conformational stability of ΔF508-CFTR. Additionally, knockdown of *RPL12* in combination with VX-809 restored ΔF508-CFTR function to ~50% of the wild-type channel in primary human airway epithelial cells. Lukacs and colleagues also observed that silencing of RPLP0, RPLP1, and RPLP2, all components of the ribosomal stalk, partially rescued ΔF508-CFTR function. Our GSEA analysis revealed that genes related to the large ribosomal subunit were significantly downregulated in our RNA-sequencing data of XL147 treated cells compared to DMSO, further supporting the hypothesis that XL147 could be rescuing ΔF508-CFTR through the silencing of ribosomal stalk proteins. Generally, the roles of ribosomal stalk proteins in disease have been enigmatic and understudied.[41] The relationship between CFTR biogenesis and the ribosomal stalk requires further investigation.

The latest clinical trials for CFTR modulators have consisted of multi-drug combinations, as it is likely that a single corrector is inefficient to restore ΔF508-CFTR maturation and function.[26] The redundancy and complexity of quality control mechanisms that detect and degrade ΔF508-CFTR likely contribute to the need for additional therapies[42–46] such as the recently FDA-approved triple combination of elexacaftor-tezacaftor-ivacaftor.[26] Indeed, XL147 also showed cooperativity when administered with C18 and cotreatment of the two small molecules yielded a significant increase in CFTR-dependent Cl^- current compared to C18 alone. C18 is an analog of the FDA-approved VX809 (Lumacaftor) and affects the biosynthetic processing of ΔF508-CFTR, while likely also inducing conformational changes that improve the gating defect.[47,48] C18 and VX-809 are not believed to act through a transcriptional

mechanism and may act as chemical chaperones for the misfolded protein. Indeed, our RNA-sequencing data of C18 and VX-809 treated cells support this hypothesis, as both small molecules induced very few differentially expressed genes when compared to DMSO. Therefore, these molecules are excellent candidates for cotreatment with small molecules that act through a different mechanism, such as the transcriptionally active XL147. The cooperativity between XL147 and C18 supports the utility of modulator cotreatment with transcriptionally active small molecules and CFTR-interacting drugs.

Although the clinical utility of XL147 as a modulator for CF requires further studies, the discovery of its effect on ΔF508-CFTR processing and function highlights the genomic signature pattern-matching strategy. Furthermore, LINCS continues to expand its database and develop new publicly available tools. The BD2K-LINCS Data Coordination and Integration Center has developed methods to connect cellular phenotypes with molecular signatures. For example, Harmonizome is a biological knowledge engine containing information about genes and proteins from 70 resources, allowing for discovery across diverse sets of omics resources.[49] Additionally, Drug Gene Budger allows for the identification of small molecules that up- or downregulate an individual gene of interest.[50] Such tools provide further opportunities for drug discovery in CF and other diseases.

ACKNOWLEDGEMENTS

The authors thank Drs. Todd Golub and Josh Bittker at the Broad Institute for providing helpful input at the outset of this project. We thank Drs. Rachel Hodos, Jennifer Bartlett, Amber Vu, Scott Ebert, and Christopher Adams for their valuable discussions and feedback. We acknowledge the support of the University of Iowa In Vitro Models and Cell Culture Core.

CONFLICT OF INTEREST

The authors declare no conflicts of interest.

AUTHOR CONTRIBUTIONS

M.D.S., S.R., A.S., A.L., R.J.B., and P.B.M. designed research. M.D.S., S.R., D.Y.B., E.A.M., A.S., and A.L. performed research. M.D.S., S.R., D.Y.B., A.A.P., and P.B.M. analyzed data. M.D.S. and P.B.M. wrote the manuscript.

DATA AVAILABILITY STATEMENT

RNA-sequencing data are available as BioProject ID PRJNA746672. Code has been placed in a public repository at https://github.com/matthewdstrub/XL147. Data required to run the code is located at https://drive.google.com/drive/u/0/folders/1Zi8ivsYDsslR_SnIMVkLpWWlbTjuVjcB and has been linked in the README.

REFERENCES

1. Riordan JR, Rommens JM, Kerem B-S, et al. Identification of the cystic fibrosis gene: cloning and characterization of complementary DNA. *Science*. 1989;245:1066-1073.
2. Denning GM, Ostedgaard LS, Welsh MJ. Abnormal localization of cystic fibrosis transmembrane conductance regulator in primary cultures of cystic fibrosis airway epithelia. *J Cell Biol*. 1992;118:551-559.
3. Kartner N, Augustinas O, Jensen TJ, Naismith AL, Riordan JR. Mislocalization of delta F508 CFTR in cystic fibrosis sweat gland. *Nat Genet*. 1992;1:321-327.
4. Pedemonte N, Lukacs GL, Du K, et al. Small-molecule correctors of defective DeltaF508-CFTR cellular processing identified by high-throughput screening. *J Clin Invest*. 2005;115:2564-2571.
5. Ramachandran S, Karp PH, Jiang P, et al. A microRNA network regulates expression and biosynthesis of wild-type and DeltaF508 mutant cystic fibrosis transmembrane conductance regulator. *Proc Natl Acad Sci U S A*. 2012;109:13362-13367.
6. Lamb J. The Connectivity Map: a new tool for biomedical research. *Nat Rev Cancer*. 2007;7:54-60.
7. Ramachandran S, Osterhaus SR, Karp PH, Welsh MJ, McCray PB Jr. A genomic signature approach to rescue DeltaF508-cystic fibrosis transmembrane conductance regulator biosynthesis and function. *Am J Respir Cell Mol Biol*. 2014;51:354-362.
8. Dyle MC, Ebert SM, Cook DP, et al. Systems-based discovery of tomatidine as a natural small molecule inhibitor of skeletal muscle atrophy. *J Biol Chem*. 2014;289:14913-14924.
9. Dudley JT, Deshpande T, Butte AJ. Exploiting drug-disease relationships for computational drug repositioning. *Brief Bioinform*. 2011;12:303-311.
10. Dudley JT, Sirota M, Shenoy M, et al. Computational repositioning of the anticonvulsant topiramate for inflammatory bowel disease. *Sci Transl Med*. 2011;3:96ra76.
11. Raghavan R, Hyter S, Pathak HB, et al. Drug discovery using clinical outcome-based Connectivity Mapping: application to ovarian cancer. *BMC Genom*. 2016;17:811.
12. Keenan AB, Jenkins SL, Jagodnik KM, et al. The library of integrated network-based cellular signatures NIH program: system-level cataloging of human cells response to perturbations. *Cell Syst*. 2018;6:13-24.
13. Subramanian A, Narayan R, Corsello SM, et al. A next generation connectivity map: L1000 platform and the first 1,000,000 profiles. *Cell*. 2017;171:1437-1452 e1417.
14. Kunzelmann K, Schwiebert EM, Zeitlin PL, Kuo WL, Stanton BA, Gruenert DC. An immortalized cystic fibrosis tracheal epithelial cell line homozygous for the delta F508 CFTR mutation. *Am J Respir Cell Mol Biol*. 1993;8:522-529.
15. Wu X, Wakefield JK, Liu H, et al. Development of a novel trans-lentiviral vector that affords predictable safety. *Mol Ther*. 2000;2:47-55.
16. Bebok Z, Collawn JF, Wakefield J, et al. Failure of cAMP agonists to activate rescued deltaF508 CFTR in CFBE41o- airway epithelial monolayers. *J Physiol*. 2005;569(Pt 2):601-615.
17. Karp PH, Moninger TO, Weber SP, et al. An in vitro model of differentiated human airway epithelia. Methods for establishing primary cultures. *Methods Mol Biol*. 2002;188:115-137.
18. Hodos RA, Strub MD, Ramachandran S, et al. Integrative chemogenomic analysis identifies small molecules that

partially rescue DeltaF508-CFTR for cystic fibrosis. *CPT Pharmacometrics Syst Pharmacol*. 2021;10:500-510.
19. Pimentel H, Bray NL, Puente S, Melsted P, Pachter L. Differential analysis of RNA-seq incorporating quantification uncertainty. *Nat Methods*. 2017;14:687-690.
20. Bray NL, Pimentel H, Melsted P, Pachter L. Near-optimal probabilistic RNA-seq quantification. *Nat Biotechnol*. 2016;34:525-527.
21. Szklarczyk D, Gable AL, Lyon D, et al. STRING v11: protein-protein association networks with increased coverage, supporting functional discovery in genome-wide experimental datasets. *Nucleic Acids Res*. 2019;47:D607-D613.
22. Woo JH, Shimoni Y, Yang WS, et al. Elucidating compound mechanism of action by network perturbation analysis. *Cell*. 2015;162:441-451.
23. Sondo E, Tomati V, Caci E, et al. Rescue of the mutant CFTR chloride channel by pharmacological correctors and low temperature analyzed by gene expression profiling. *Am J Physiol Cell Physiol*. 2011;301:C872-C885.
24. Veit G, Oliver K, Apaja PM, et al. Ribosomal stalk protein silencing partially corrects the DeltaF508-CFTR Functional Expression Defect. *PLoS Biol*. 2016;14:e1002462.
25. Clancy JP, Rowe SM, Accurso FJ, et al. Results of a phase IIa study of VX-809, an investigational CFTR corrector compound, in subjects with cystic fibrosis homozygous for the F508del-CFTR mutation. *Thorax*. 2012;67:12-18.
26. Middleton PG, Mall MA, Dřevínek P, et al. Elexacaftor-tezacaftor-ivacaftor for cystic fibrosis with a single Phe508del allele. *N Engl J Med*. 2019;381:1809-1819.
27. Keating D, Marigowda G, Burr L, et al. VX-445-tezacaftor-ivacaftor in patients with cystic fibrosis and one or two phe508del alleles. *N Engl J Med*. 2018;379:1612-1620.
28. Douros K, Loukou I, Doudounakis S, Tzetis M, Priftis KN, Kanavakis E. Asthma and pulmonary function abnormalities in heterozygotes for cystic fibrosis transmembrane regulator gene mutations. *Int J Clin Exp Med*. 2008;1:345-349.
29. Heijerman HGM, McKone EF, Downey DG. et al. Efficacy and safety of the elexacaftor plus tezacaftor plus ivacaftor combination regimen in people with cystic fibrosis homozygous for the F508del mutation: a double-blind, randomised, phase 3 trial. *Lancet*. 2019;394:1940-1948.
30. Davidson BL, McCray PB Jr. Current prospects for RNA interference-based therapies. *Nat Rev Genet*. 2011;12:329-340.
31. Pesce E, Gorrieri G, Sirci F, et al. Evaluation of a systems biology approach to identify pharmacological correctors of the mutant CFTR chloride channel. *J Cyst Fibros*. 2016;15:425-435.
32. Hegde RN, Parashuraman S, Iorio F, et al. Unravelling druggable signalling networks that control F508del-CFTR proteostasis. *Elife*. 2015;4:e10365.
33. Van Goor F, Straley KS, Cao D, et al. Rescue of DeltaF508-CFTR trafficking and gating in human cystic fibrosis airway primary cultures by small molecules. *Am J Physiol Lung Cell Mol Physiol*. 2006;290:L1117-L1130.
34. Foster P, Yamaguchi K, Hsu PP, et al. The selective PI3K inhibitor XL147 (SAR245408) inhibits tumor growth and survival and potentiates the activity of chemotherapeutic agents in preclinical tumor models. *Mol Cancer Ther*. 2015;14:931-940.
35. Reilly R, Mroz MS, Dempsey E, et al. Targeting the PI3K/Akt/mTOR signalling pathway in Cystic Fibrosis. *Sci Rep*. 2017;7:7642.
36. Trzcinska-Daneluti AM, Nguyen L, Jiang C, et al. Use of kinase inhibitors to correct DeltaF508-CFTR function. *Mol Cell Proteomics*. 2012;11:745-757.
37. Trzcińska-Daneluti AM, Chen A, Nguyen L, et al. RNA interference screen to identify kinases that suppress rescue of deltaf508-CFTR. *Mol Cell Proteomics*. 2015;14:1569-1583.
38. Tuo B, Wen G, Zhang Y, et al. Involvement of phosphatidylinositol 3-kinase in cAMP- and cGMP-induced duodenal epithelial CFTR activation in mice. *Am J Physiol Cell Physiol*. 2009;297:C503-C515.
39. Jung HJ, Kwon TH. Membrane trafficking of collecting duct water channel protein AQP2 regulated by Akt/AS160. *Electrolyte Blood Press*. 2010;8:59-65.
40. Robertson SD, Matthies HJG, Owens WA, et al. Insulin reveals Akt signaling as a novel regulator of norepinephrine transporter trafficking and norepinephrine homeostasis. *J Neurosci*. 2010;30:11305-11316.
41. Liljas A, Sanyal S. The enigmatic ribosomal stalk. *Q Rev Biophys*. 2018;51:e12.
42. Pedemonte N, Galietta LJ. Pharmacological correctors of mutant CFTR mistrafficking. *Front Pharmacol*. 2012;3:175.
43. Thibodeau PH, Richardson JM 3rd, Wang W, et al. The cystic fibrosis-causing mutation deltaF508 affects multiple steps in cystic fibrosis transmembrane conductance regulator biogenesis. *J Biol Chem*. 2010;285:35825-35835.
44. Galietta LJ. Managing the underlying cause of cystic fibrosis: a future role for potentiators and correctors. *Paediatr Drugs*. 2013;15:393-402.
45. Okiyoneda T, Veit G, Dekkers JF, et al. Mechanism-based corrector combination restores DeltaF508-CFTR folding and function. *Nat Chem Biol*. 2013;9:444-454.
46. Kalid O, Mense M, Fischman S, et al. Small molecule correctors of F508del-CFTR discovered by structure-based virtual screening. *J Comput Aided Mol Des*. 2010;24:971-991.
47. Wang Y, Loo TW, Bartlett MC, Clarke DM. Additive effect of multiple pharmacological chaperones on maturation of CFTR processing mutants. *Biochem J*. 2007;406:257-263.
48. He L, Kota P, Aleksandrov AA, et al. Correctors of DeltaF508 CFTR restore global conformational maturation without thermally stabilizing the mutant protein. *FASEB J*. 2013;27:536-545.
49. Rouillard AD, Gundersen GW, Fernandez NF, et al. The harmonizome: a collection of processed datasets gathered to serve and mine knowledge about genes and proteins. *Database (Oxford)*. 2016;2016:baw100.
50. Wang Z, He E, Sani K, et al. Drug Gene Budger (DGB): an application for ranking drugs to modulate a specific gene based on transcriptomic signatures. *Bioinformatics*. 2019;35:1247-1248.

SUPPORTING INFORMATION

Additional supporting information may be found in the online version of the article at the publisher's website.

How to cite this article: Strub MD, Ramachandran S, Boudko DY, et al. Translating *in vitro* CFTR rescue into small molecule correctors for cystic fibrosis using the Library of Integrated Network-based Cellular Signatures drug discovery platform. *CPT Pharmacometrics Syst Pharmacol*. 2022;11:240-251. doi:10.1002/psp4.12751